

Experimental and Numerical Investigation of Aluminum Beams: Flexural Behavior Section Shape Effect

Sa'ad Fahad Resan^{*1a}, Nabeel Abdulrazzaq Jasim^{2b}

¹ Civil Engineering Department, Engineering College, University of Misan, Amarah, Iraq.

² Civil Engineering Department, Engineering College, University of Basrah, Basrah, Iraq.

*Corresponding author E-mail: sadresan@uomisan.edu.iq

(Received 3 March, Revised 22 July, Accepted 16 Aug)

Abstract: Advanced technology and other aspects of life aim to use the available and efficient materials. Due to their high strength-to-weight ratio and durability, aluminum alloys are used in a variety of structural engineering applications. This paper describes the experimental and numerical flexural behavior investigation of the aluminum beams. The main variables considered in the study are related to section shape, which are the shape configuration, depth, and thickness of the aluminum section. The finite element three dimensional models are used to analyze the tested beams in order to check the ability of the models to predict the overall behavior and to obtain more information about the stresses and strains that developed. The results show that the larger the value of the section shape factor, the fiber is still in the elastic range, and the smaller the plastic deformation of the beam. And the web plates slenderness ratio has a significant influence on the load-deflection relationship because of local deformation as well as the plastic deformation of box beams is relatively smaller than that of the I-section beam. The constraint of the flange for box beams is greater than that for I-section beams. Besides, the adopted nonlinear numerical modeling gives acceptable agreement with the experimental results besides the load-deflection responses, the ultimate strength convergence ratios varied between 1.1-0.93.

Keywords: Aluminium alloy, Aluminium beam, Flexural behaviour, Finite element model, and section shape.

1. Introduction

Aluminum is the third most common element in the earth's crust, coming after oxygen and silicon. It makes up 8% of the crust's total mass and is the most abundant metal [1]. Pure aluminum is weak, with a tensile strength ranging from about 90 to 140 N/mm² depending on the temper. It is employed for electrical conductors and for domestic products (such as pans, cans, and packaging), but for serious structural use it has to be strengthened by alloying. The strongest alloys have a tensile strength of over 500 N/mm². Because of its low values, pure aluminum is not suitable for structural applications because of its low mechanical characteristics. In order for aluminum to be useful as a structural metal, it was essential to develop suitable Alloys, However, many alloys are available with a large variety of excellent mechanical and physical qualities. The appropriate alloy depends on the specific application. The 6xxx series alloys are the most useful for structural applications because of their combination of strength, corrosion resistance, and weldability [1]. There are around ten basic alloys from which wrought material (plate, sheet, and sections) is produced. Unfortunately, each of these alloys appears in a vast range of different versions, so the full list of actual specifications is long. The newcomer, therefore finds material selection less simple than it is in structural steel, and there is also the alloy numbering system to contend with [1]. There are many advantages of using aluminum alloys, such as high strength-to-weight ratio, lightness, corrosion resistance, good workability and ease of production. Aluminum can also be recycled, which gives environmental advantages.

However, many alloys are available with a large variety of excellent mechanical and physical qualities. The appropriate alloy depends on the specific application. The 6xxx series alloys are the most useful for structural applications because of their combination of strength, corrosion resistance, and weldability. Alloys in this group contain magnesium and silicon in proportions that form magnesium silicide (Mg₂Si).

These alloys have a good balance of corrosion resistance and strength. The 6xxx series alloys are also very readily extruded, so they constitute the majority of extrusions produced and are used extensively in building, construction, and other structural applications [2].

The main kinds of structural applications belong to the following groups [3]: long-span roof systems, structures located in inaccessible places far from the fabrication shop, structures situated in corrosive or humid environments, structures having moving parts, structures for special purposes, for which maintenance operations are particularly difficult and must be limited, as in case of masts, lighting towers, and sign motorway portals. An example of structural application of aluminum alloys is shown in Figure 1.



Fig.1 Installation of an aluminum deck on aluminum beams [1]

Aluminum is easily the second most important structural metal, yet few designers seem to know much about it. Since the 1940s, aluminum has rapidly become more important. Researchers have been slow to investigate what it has to offer and how to design with it, and many related structural topics have been studies [4-19]. This study aims to a comparative analysis related to section shape effects on aluminum beam flexural bending behavior. The main variables considered in the study were the aluminum section shape, depth and thickness of the aluminum section.

2. Experimental Program

This section describes the experimental work objectives, details of specimens, material properties, the instrumentation utilized, and the testing procedures.

2.1. Aluminum section details

A structural aluminum alloy section produced by the Jordanian aluminum industry has been used in this investigation. The geometrical details are shown in Table 1, and Figure 2 exhibit aluminum section details used in this study.

2.2 Mechanical Properties

The main ingredients of the used structural aluminum alloys are determined in chemical laboratory as shown in Table 2. The mechanical properties of the aluminum were determined by using a tensile coupon. The tensile coupons were taken from the center of the web plate in the longitudinal direction of the aluminum beams.

Table 1 Details of aluminum beams

No.	Code	Section	Weight Kg/m.l	Full depth, D mm	length, mm	Flange width, B mm	Flange thicken- ss, tf	Web thickenss, tw mm	Aa mm ²	Calculated Ia mm ⁴
1	S1	20x5x0.4 cm	5.12	200	1200	50	4	4	1936	8560725
2	S2	10x5x0.4 cm	3	100	1200	50	4	4	1136	1441259
3	S3	10x5x0.3 cm	2.29	100	1200	50	3	3	864	1121192
4	S4	16x10-6x0.5 cm	4.87	160	1200	100,60	6	5	1800	4943467

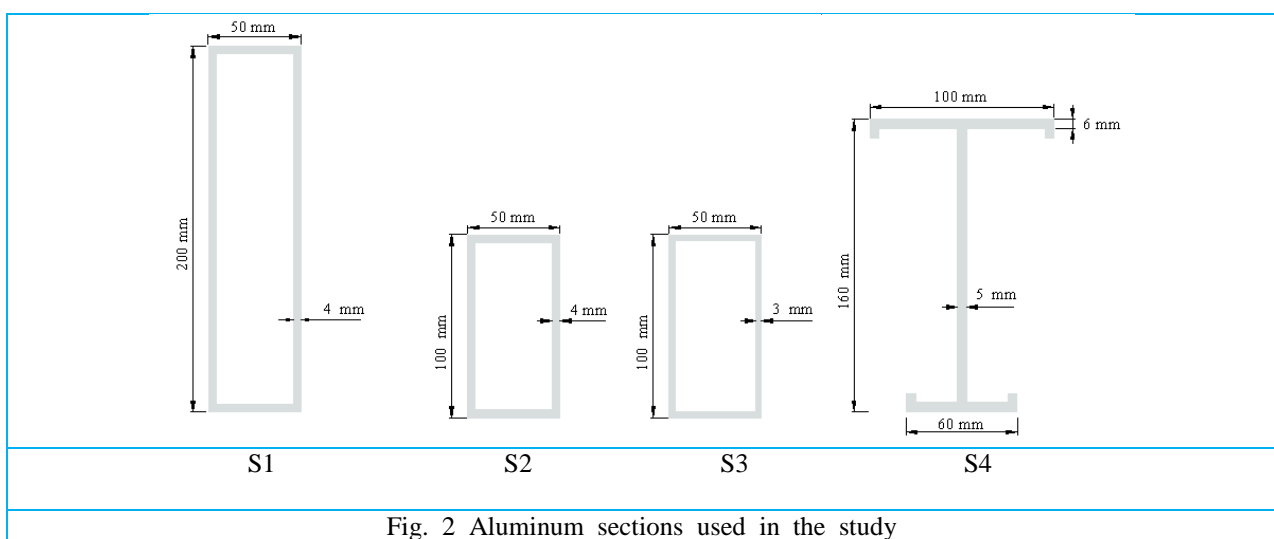


Fig. 2 Aluminum sections used in the study

The tensile coupons were prepared and tested according to the American Society for Testing and Materials standard (B557M-ASTM 2003-Standard: Test Methods of Tension Testing Wrought and Cast Aluminum- and Magnesium-Alloy Products) [20]. In the tensile test, 12.5 mm wide coupons of 50 mm gauge length were used as shown in Fig. (3-3). They were tested under direct tension by a 5 kN capacity Bench-Top testing machine model BT-1000. The material properties obtained from the tensile tests are summarized in Table 3, which includes the measured initial Young's modulus (E_0), the static 0.2% tensile proof stress $f_{0.2}$, the static tensile strength f_u , and the elongation after fracture. This is typically measured on a gauge-length of 50 mm and gives a crude indication of ductility. The compressive proof stress was not recorded, and it is normally assumed to be the same as in tension [5].

Figure 3 shows samples of the stress-strain curve for the box and I – section, respectively. Figure shows failed tensile test coupons and test arrangement, respectively. Table 2 shows the weight percentage of the main ingredients of the used structural aluminum alloys.

Table 2 Main ingredients of structural aluminum alloy

Chemical elements	Composition, wt%	
	Box section	I section
Al	95.02	95.91
Mg	0.32	0.21
Si	0.35	0.33

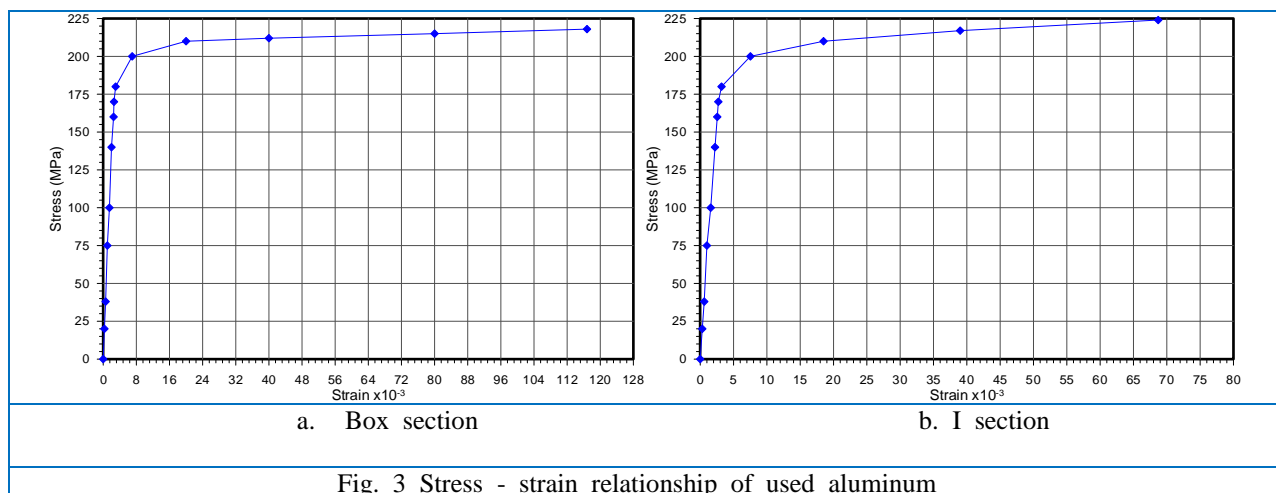


Fig. 3 Stress - strain relationship of used aluminum

Table 3 Mechanical Properties

Section style	Specimens	$f_{0.2}$ yield stress (MPa)	Ultimate stress (MPa)	E (GPa)	Fracture elongation (%)	Specific elongation[5] (%)
Box	a1	184.66	224.42	64.65	6.87	6-14
	a2	186.76	220.58	63.37	6.98	
	a3	182.29	225.5	65.54	7.09	
I-Shape	b1	192.24	219.11	68.01	11.9	6-14
	b2	188.35	221.23	67.97	12.11	
	b3	187.76	226.32	66.14	11.68	

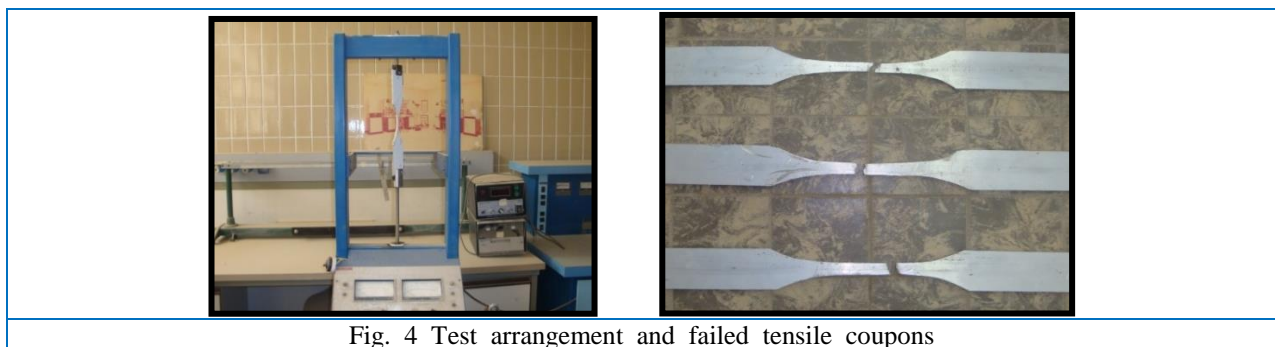


Fig. 4 Test arrangement and failed tensile coupons

During testing, the main characteristics of the structural behavior of the specimens were measured at every stage of loading. For each test, the ultimate loads were recorded. Also, for each load increment, strains were recorded. The specimens tested for flexural strength were tested under a third point arrangement. Mechanical dial gauges were used to measure deflection while mechanical strain – gauge was used to measure strains at midspan of the member by using demic points (locating discs having 6.3 mm diameter) with 5 cm gauge length. All beam specimens were tested by the Universal Testing Machine (TORSEE) 200-ton capacity.

3. Finite Element Analysis

In the present section, the tested beams have been analyzed using three-dimensional finite element models. The main objectives of the analysis are to check the accuracy of the adopted finite element models to predict the overall behavior of the tested beams and to get more information about the stresses and strains developed in the beams. In nonlinear analysis, the total load applied to a finite element model

is divided into a series of load increments called load steps. After the completion of each incremental solution, the stiffness matrix of the model is adjusted to reflect nonlinear changes in structural stiffness before proceeding to the next load increment. The ANSYS program (ANSYS version 11.0) [21] uses Newton-Raphson equilibrium iterations for updating the model stiffness. Figure .5 shows the considering Finite element models.

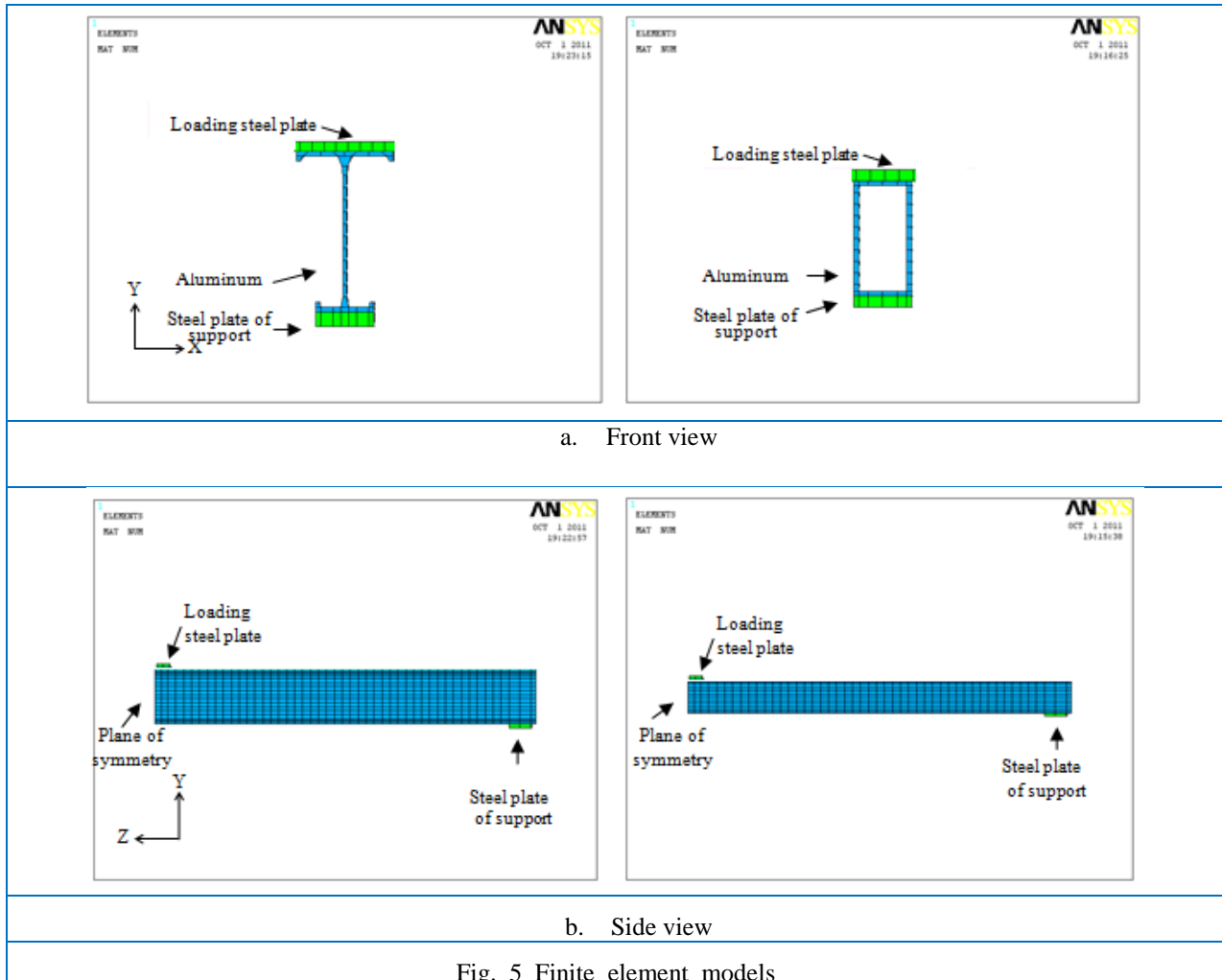


Fig. 5 Finite element models

It has been found that the simulation of the applied load and the supports has a significant effect on the results of the finite element analysis. To simulate the applied loads, loads (P) were distributed equally among the node lines within the loading plate and ($P/2$) on the edge nodes lines. Displacement boundary conditions are needed to constrain the model to get a unique solution. To ensure that the model acts in the same way as the experimental beam, boundary conditions need to be applied at points of symmetry, and where the supports and loadings exist.

4. Results and Discussion

4.1 Experimental Analysis

The tests included four beam specimens of different cross-sectional geometries, three of them of box sections with various details and one I- section. They are made of the same aluminum alloy and these sections are used as metal components in composite beams. The test specimens were of 1.2 m long, with a clear span of 1.1 m. All beams were loaded with a point load at mid-span. The load on beams is applied monotonically in increments. These increments were reduced in magnitude as the load reached its

ultimate value. The maximum load recorded by the testing machine is considered as the ultimate load. The results of tested aluminum beams are summarized in Table 4. Aluminum alloys are typical nonlinear materials, and consequently bending members made of this material exhibit a nonlinear behavior as shown in Figure 6. The followings may be stated:

1-Influence of the shape factor on the load-deflection relationship (The shape factor indicates how much more load can be carried by the structural shape than by the same mass of material with a square cross section, equals to $(12 I/A^2)$). When the exterior fiber of the section yields, the interior fiber is still in the elastic range. The larger the value of section the shape factor, as for (S1) the more the fiber is still in the elastic range, and the smaller the plastic deformation of the beam.

2-The web slenderness ratio of the tubular sections varies from 25 to 33.34 for (S2) and (S3), respectively and this leads to flexural ductility (the ratio of deflection at ultimate load to the deflection corresponding to load at the end of the linear stage) changing between (2.5) and (2.1), so the web plates slenderness ratio has a significant influence on the load-deflection relationship because of local deformation.

3-The plastic deformation of box beams is relatively smaller than that of I-section beam (S4). The constraint of the flange for box beams is greater than for I-section beams, since the flange of a box beam is insensitive to the local initial out-of-flatness imperfections.

Figure 7 shows the strain distribution across the depth of tested aluminum beams for intermediate load values in the linear stage and the ultimate load. In all specimens, measured strains are less than the percentage elongation obtained in the tension test which is (0.07) for box section and (0.12) for I-section, and larger than yield strain of (0.014) for box section and (0.016) for I-section.

In general, all beams exhibited local buckling during failure which a property of slender metal sections. When the aluminum section is under compression and owing to the small thickness, local buckling which is an instability phenomenon in the compressed parts of the section is more likely to occur, Figure 8.

Table 4 Experimental results

No.	Code	Shape factor ($12 I/A^2$)	P_u (kN)	M_u (kN.m)	Δ_u (mm)	$\epsilon \times 10^{-3}$
1	S1	27.4	95.12	26.16	7.67	9.6
2	S2	13.4	28.44	7.82	16	46.4
3	S3	18	21.87	6.01	20	59.2
4	S4	18.3	77.27	21.25	14.01	69

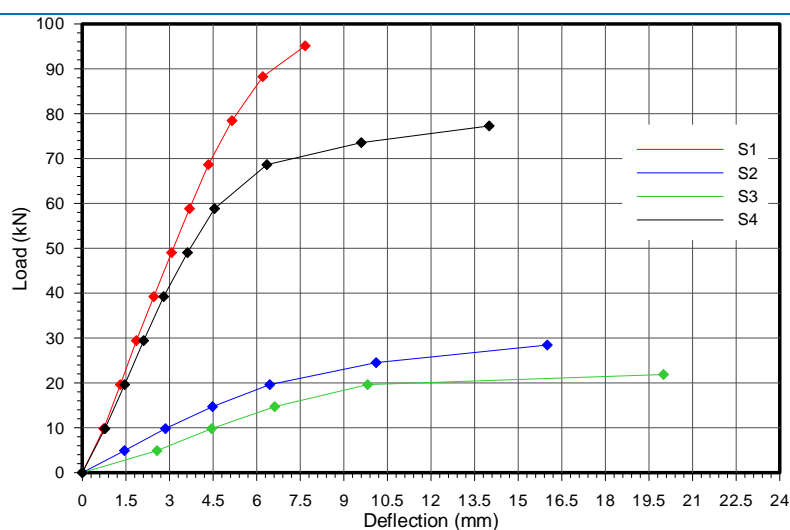
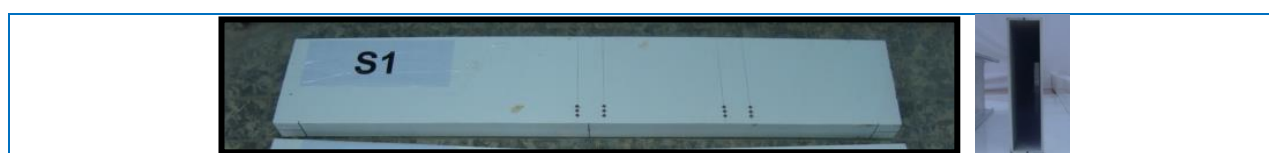
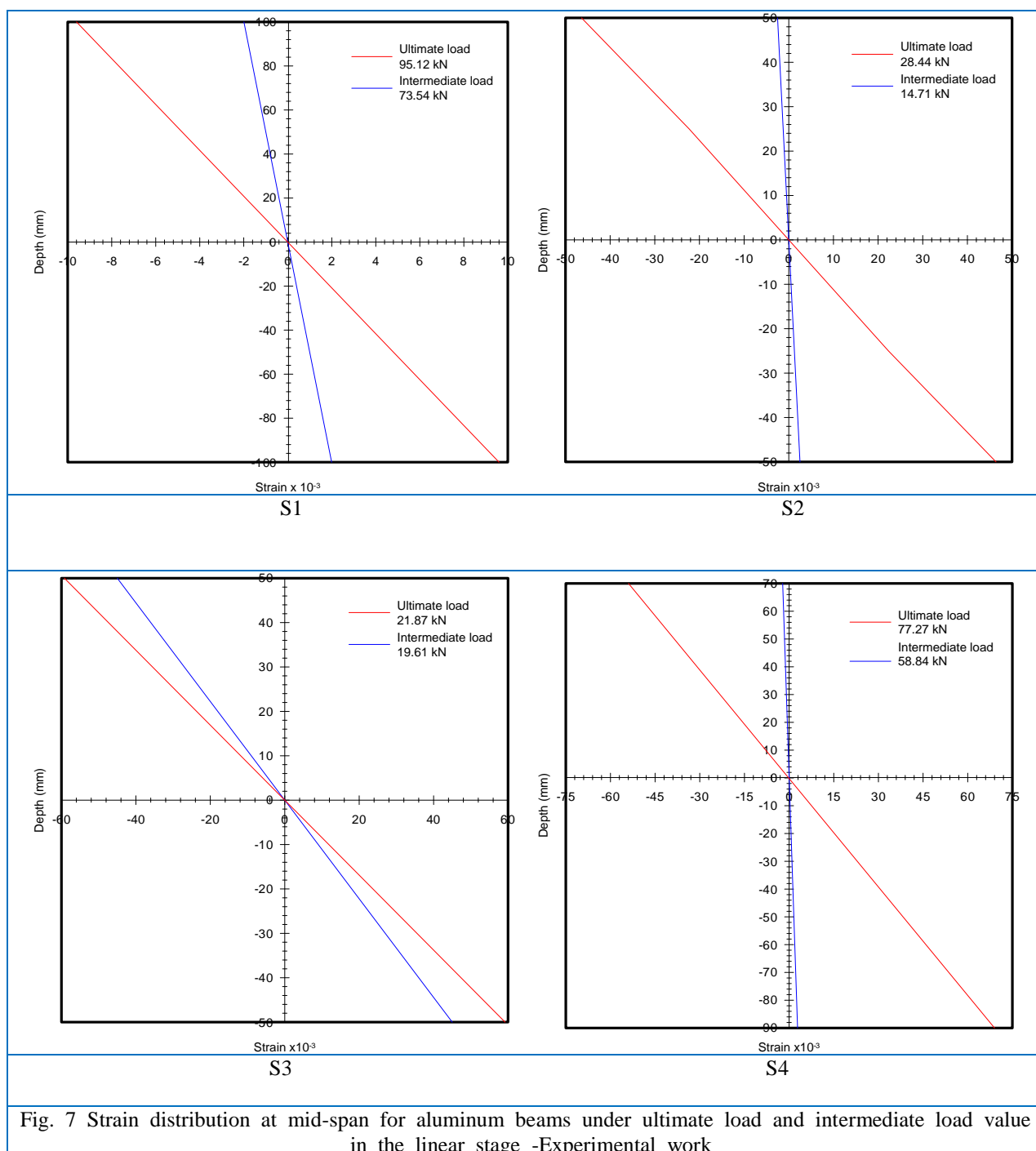


Fig. 6 Variation of mid-span deflection with load for aluminum beams – Experimental work



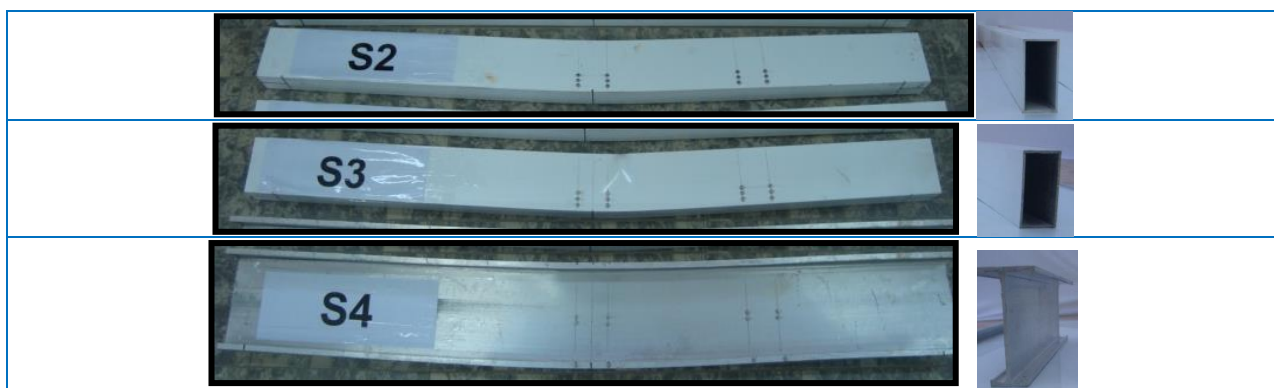


Fig. 8 Aluminum beams after failure

4.2 Numerical Analysis

In the physical test under load control, the collapse of a structure occurs when no further load increment can be sustained. This is usually indicated in the numerical test by successively increasing iterative displacements and continuous growth in the dissipated energy. Hence, the convergence of the iterative process cannot be achieved. So the values of ultimate load obtained are theoretically attributed to the solution divergence [22]. The ultimate load for each beam as tested and calculated by using the finite element method is shown in Table 5. The finite element model by using ANSYS package is found to give ultimate loads closer to the experimental values. The ratios of predicted to experimental values of ultimate load are 0.93 to 1.1 of an average of 1.02 for aluminum beams with 1.2 m length. Considering the strain hardening portion of the stress-strain relationship of aluminum in the theoretical evaluation of ultimate loads may be the reason behind obtaining very close values for aluminum beams.

Figure 9 illustrates the load-deflection relationships, for tested beams. The experimental relationships alongside the theoretical ones, are collected for each beam. The finite element analysis is found to give close relationships to experimental results. Table 6 illustrates the comparison between the experimental results and the theoretical ones for deflections at ultimate and service loads (2/3 the ultimate loads).

The load-strain relationships for all beams are depicted in Figure 10. Table 7 illustrates the comparison between the experimental results and the theoretical ones. Figure 11 reveals the typical deformed shape and contours for longitudinal strain distribution at ultimate load.

Table 5 Ultimate and service loads of tested beams

No.	Beams designation	Ultimate load (kN)		Service load (kN)		Ultimate Pexp/Pth
		Experimental (Pexp)	Theoretical (Pth)	Experimental (Pexp)	Theoretical (Pth)	
1	S1	95.12	86.73	63.41	57.82	1.10
2	S2	28.44	27.30	18.96	18.20	1.04
3	S3	21.87	21.98	14.58	14.65	0.99
4	S4	77.27	82.80	51.51	55.20	0.93

Table 6 Deflections of tested beams

No.	Beams designation	Deflection at ultimate load (mm)	Deflection at service load (mm)
-----	-------------------	----------------------------------	---------------------------------

		Experimental (d_{exp})	Theoretical (d_{th})	d_{exp}/d_{th}	Experimental (d_{exp})	Theoretical (d_{th})	d_{exp}/d_{th}
1	S1	7.67	10.26	0.75	3.98	3.92	1.02
2	S2	16	41.00	0.39	6.235	7.00	0.89
3	S3	20	41.12	0.49	6.561	5.90	1.11
4	S4	14.01	36.96	0.38	3.803	4.60	0.83

Table 7 Comparison of experimental and theoretical strain for tested beams

No.	Beams designation	Compressive strain at ultimate load ($\times 10^{-3}$)		Tensile strain in at ultimate load ($\times 10^{-3}$)	
		Experimental	Theoretical	Experimental	Theoretical
1	S1	-	14.28	9.60	12.82
2	S2	-	58.53	46.41	58.00
3	S3	-	141.60	59.00	137.13
4	S4	-	50.94	69.00	123.09

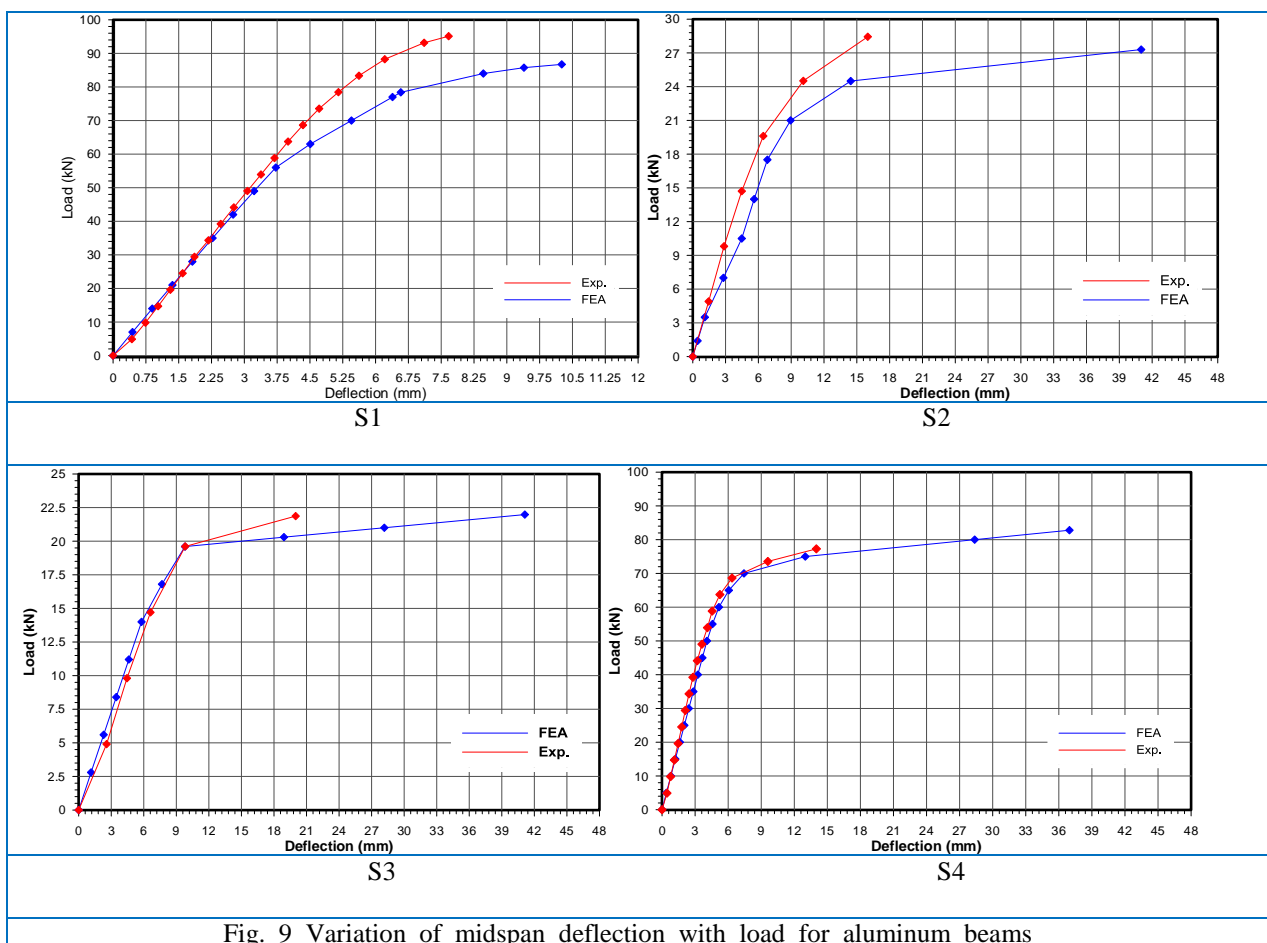


Fig. 9 Variation of midspan deflection with load for aluminum beams

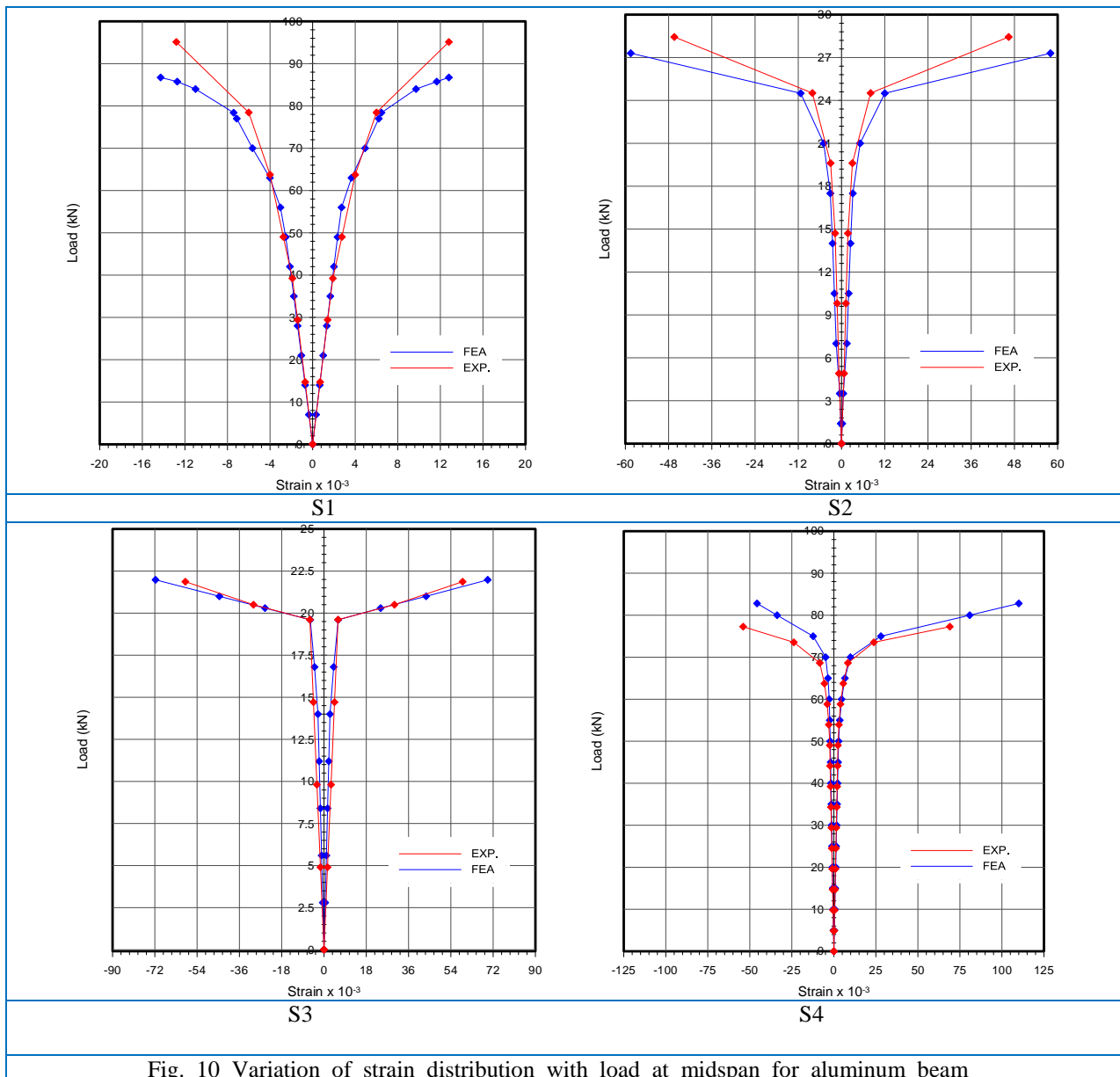
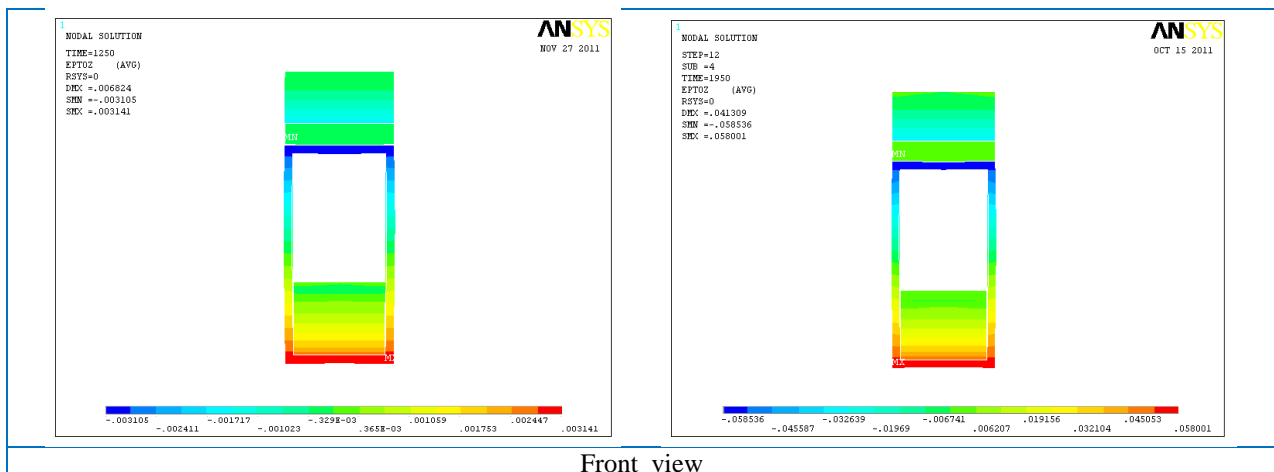
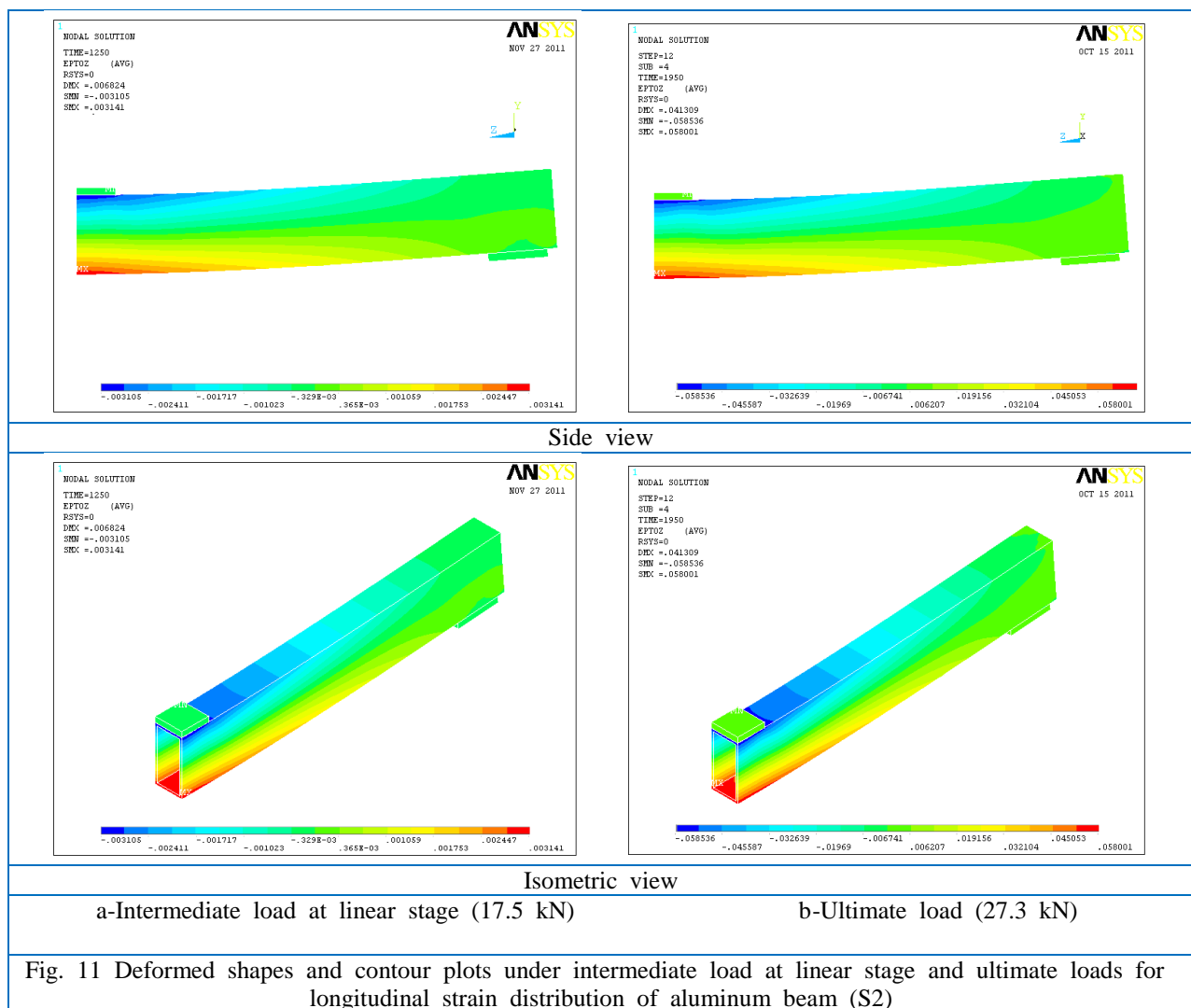


Fig. 10 Variation of strain distribution with load at midspan for aluminum beam



Front view



5. Conclusions

1. The influence of the shape factor on the load-deflection response is assigned. When the exterior fiber of the section yields, the interior fiber is still in the elastic range. The larger the value of the section shape factor, as for (S1), the more the fiber is still in the elastic range and the smaller the plastic deformation of the beam.
- 2-The web slenderness ratio of the tubular sections varies from 25 to 33.34 for (S2) and (S3), respectively, and this leads the flexural ductility changing between (2.5) and (2.1), so the web plates slenderness ratio has a significant influence on the load-deflection relationship because of local deformation.
- 3-The plastic deformation of box beams is relatively smaller than that of the I-section beam (S4). The constraint of the flange for box beams is greater than that for I-section beams since the flange of a box beam is insensitive to the local initial out-of-flatness imperfections.
4. In all specimens, measured strains are less than the percentage elongation obtained in the tension test, which is (0.07) for box section and (0.12) for I-section, and larger than the yield strain of (0.014) for box section and (0.016) for I-section.

5. In general, all beams exhibited local buckling during failure, which is property of slender metal sections. When the aluminum section is under compression and owing to the small thickness, local buckling which is an instability phenomenon in the compressed parts of the section is more likely to occur.

6. Nonlinear finite element solution by (ANSYS version 11.0) package program using three -dimensional elements for modeling the aluminum beam gives acceptable agreement with the experimental results besides the load-deflection responses.

Acknowledgments: The researcher would like to thank everyone who has helped us and convey their sincere gratitude.

Author Contributions: The authors contributed to all parts of the current study.

Funding: This study received no external funding .

Conflicts of Interest: The authors declare no conflict of interest.

References

- [1] John Dwight, (1999) "Aluminum Design and Construction", First published, University of Cambridge, London.
- [2] Randolph K. and Robert L. Ferry, "Aluminum structures; A Guide to Their Specifications and Design", Second edition, New York.
- [3] Federico M. Mazzolani, (2002) "The Structural use of Aluminum: Design and Application", *Fourth International Conference on Steel and Aluminum Structures – Light Weight steel and aluminum structures*, pp. 475-486, Department of Civil & Environmental Engineering, Helsinki University of Technology, Finland, June.
- [4] Brown and Evans, (1994) "Theoretical and Experimental Investigation of the Collapse Behavior of Transversely Stiffened Aluminum Alloy Plate Girders", *Journal of Thin- Walled Structures*, Vol.18, pp. 225-246.
- [5] Landolfo and Mazzolani, (1997) "Different Approaches in the Design of Slender Aluminum Alloy Sections" , *Journal of Thin- Walled Structures*, Vol. 27, No. I, pp. 85-102.
- [6] Mazzolani and Piluso, (1997) "Prediction of the Rotation Capacity of Aluminum Alloy Beams", *Journal of Thin- Walled Structures*, Vol. 27, No. I, pp. 103-116.
- [7] Moen, Hopperstad, and Langseth, (1999) "Rotational Capacity of Aluminum Beams under Moment Gradient, I:Experiments", ASCE, *Journal of Structural Engineering*, Vol. 125, No. 8.
- [8] Matteis, Moen, Langseth, Landolfo, Hopperstad, and Mazzolani, (2001) "Cross-Sectional Classification for Aluminum Beams - parametric Study", *Journal of Structural Engineering*, Vol. 127, No. 3, March, pp. 271-279.
- [9] Matteis, Landolfo, Manganiello, and Mazzolani, (2004) "Inelastic Behavior of I-Shaped Aluminum Beams: Numerical Analysis And Cross-Sectional Classification", *Journal of Computers and Structures*, Vol. 82, pp. 2157–2171.
- [10] Ji-Hua Zhu1 and Ben Young, (2006) "Experimental Investigation of Aluminum Alloy Thin-Walled Tubular Members in Combined Compression and Bending", *Journal of Structural Engineering*, Vol. 132, No. 12, pp.1955-1966.
- [11] Manganiello, Matteis, and Landolfo, (2006) "Inelastic Flexural Strength of Aluminum Alloys Structures", *Journal of Engineering Structures*, Vol. 28, pp. 593–608.
- [12] Cheng Ming, Shi Yongjiu and Wang Yuanqing, (2006) "Inelastic Deformation Analysis of Aluminum Bending Members", *Tsinghua Science and Technology* , Vol. 11, No. 6, pp648-656.
- [13] Davies and Roberts, (1999) "Resistance of Welded Aluminum alloy Plate Girders to Shear and Patch Loading", *Journal of Structural Engineering*, Vol. 125, No. 8, pp. 930-931.
- [14] Koltsakis and Preftitsi, (2008) "Numerical Investigation of The Plastic Behavior of Short Welded Aluminum Double-T Beams", *Journal of Engineering Structures*, Vol. 30, pp.2022–2031.
- [15] Wanga, Hopperstada, Lademoa and Larsen, (2007) "Finite Element Modeling of Welded Aluminum Members Subjected to Four-Point Bending", *Journal of Thin-Walled Structures*, Vol. 45, pp. 307–320.

-
- [16] Ben Young, Feng Zhou, (2008) "Aluminum Tubular Sections Subjected to Web Crippling - Part II: Proposed Design Equations", *Journal of Thin-Walled Structures*, Vol. 46, pp. 352-361.
 - [17] Bambach, (2008) "Behavior and Design of Aluminum Hollow Sections Subjected to Transverse Blast Loads", *Journal of Thin-Walled Structures*, Vol. 46, pp. 1370-1381.
 - [18] Feng Zhou, Ben Young, and Xiao Ling Zhao, (July 2009) "Tests and Design of Aluminum Tubular Sections Subjected to Concentrated Bearing Load", *Journal of Structural Engineering*, Vol. 135, No. 7, pp. 806-817.
 - [19] Ji-Hua Zhu1 and Ben Young, (2009) "Design of Aluminum Alloy Flexural Members Using Direct Strength Method", ASCE, *Journal of Structural Engineering*, Vol. 135, No. 5, May 1, pp. 558-566.
 - [20] American Society of Testing and Material (ASTM) (2003). "Standard: Test Methods of Tension Testing Wrought and Cast Aluminum- and Magnesium-Alloy Products". *ASTM B557M*, West Conshohocken, PA.
 - [21] ANSYS, (2007) "Analysis Guide", Version 11, *Swanson Analysis System, Inc.*
 - [22] Aussi A. N., (2009) "Presstressed Fiber Reinforced Polymer (FRP) for Strengthening of Concrete Members", Ph.D thesis, University of Baghdad, College of Engineering, Civil Engineering department.